MICROSCOPE Mission: final results of the test of the equivalence principle

Pierre Touboul, Gilles Métris, Manuel Rodrigues, Joel Bergé, Alain Robert, Quentin Baghi, Yves André, Judicaël Bedouet, Damien Boulanger, Stefanie Bremer, et al.

▶ **To cite this version:**

Pierre Touboul, Gilles Métris, Manuel Rodrigues, Joel Bergé, Alain Robert, et al.. *MICROSCOPE* Mission: final results of the test of the equivalence principle. Physical Review Letters, 2022, 129 (12), pp.121102. 10.1103/PhysRevLett.129.121102 . hal-03781337

HAL Id: hal-03781337
https://hal.science/hal-03781337

Submitted on 21 Sep 2022

HAL is a multi-disciplinary open access archive for the deposit and dissemination of scientific research documents, whether they are published or not. The documents may come from teaching and research institutions in France or abroad, or from public or private research centers.

L'archive ouverte pluridisciplinaire **HAL**, est destinée au dépôt et à la diffusion de documents scientifiques de niveau recherche, publiés ou non, émanant des établissements d'enseignement et de recherche français ou étrangers, des laboratoires publics ou privés.

Editors' Suggestion | Featured in Physics

MICROSCOPE Mission: Final Results of the Test of the Equivalence Principle

Pierre Touboul,[1,*] Gilles Métris,[2,†] Manuel Rodrigues,[3,‡] Joel Bergé,[3] Alain Robert,[4] Quentin Baghi,[2,3,§] Yves André,[4] Judicaël Bedouet,[5] Damien Boulanger,[3] Stefanie Bremer,[6,‖] Patrice Carle,[1] Ratana Chhun,[3] Bruno Christophe,[3] Valerio Cipolla,[4] Thibault Damour,[7] Pascale Danto,[4] Louis Demange,[2] Hansjoerg Dittus,[8] Océane Dhuicque,[3] Pierre Fayet,[9] Bernard Foulon,[3] Pierre-Yves Guidotti,[4,¶] Daniel Hagedorn,[10] Emilie Hardy,[3] Phuong-Anh Huynh,[3] Patrick Kayser,[3] Stéphanie Lala,[1] Claus Lämmerzahl,[6] Vincent Lebat,[3] Françoise Liorzou,[3] Meike List,[6,‖] Frank Löffler,[10] Isabelle Panet,[11] Martin Pernot-Borràs,[3] Laurent Perraud,[4] Sandrine Pires,[12] Benjamin Pouilloux,[4,**] Pascal Prieur,[4] Alexandre Rebray,[3] Serge Reynaud,[13] Benny Rievers,[6] Hanns Selig,[6,††] Laura Serron,[2] Timothy Sumner,[14] Nicolas Tanguy,[3] Patrizia Torresi,[4] and Pieter Visser[15]

[1]*ONERA, Université Paris Saclay, F-91123 Palaiseau, France*
[2]*Université Côte d'Azur, Observatoire de la Côte d'Azur, CNRS, IRD, Géoazur, 250 avenue Albert Einstein, F-06560 Valbonne, France*
[3]*DPHY, ONERA, Université Paris Saclay, F-92322 Châtillon, France*
[4]*CNES Toulouse, 18 avenue Edouard Belin—31401 Toulouse Cedex 9, France*
[5]*ONERA, Université de Toulouse, F-31055 Toulouse, France*
[6]*ZARM, Center of Applied Space Technology and Microgravity, University of Bremen, Am Fallturm, D-28359 Bremen, Germany*
[7]*IHES, Institut des Hautes Etudes Scientifiques, 35 Route de Chartres, 91440 Bures-sur-Yvette, France*
[8]*DLR, Köln headquarters, Linder Höhe, 51147 Köln, Germany*
[9]*Laboratoire de physique de l'Ecole normale supérieure, ENS, Université PSL, CNRS, Sorbonne Université, Université de Paris, F-75005 Paris, France, and CPhT, Ecole polytechnique, IPP, F-91128 Palaiseau, France*
[10]*PTB, Physikalisch-Technische Bundesanstalt, Bundesallee 100, 38116 Braunschweig, Germany*
[11]*IPGP, 35 rue Hélène Brion, 75013 Paris, France*
[12]*Université Paris Saclay et Université de Paris, CEA, CNRS, AIM, F-91190 Gif-sur-Yvette, France*
[13]*Laboratoire Kastler Brossel, Sorbonne Université, CNRS, ENS-PSL Université, Collège de France, 75252 Paris, France*
[14]*Blackett Laboratory, Imperial College London, Prince Consort Road, London SW7 2AZ, United Kingdom*
[15]*Faculty of Aerospace Engineering, Delft University of Technology, Kluyverweg 1, 2629 HS Delft, Netherlands*

(Received 27 January 2022; revised 10 March 2022; accepted 30 March 2022; published 14 September 2022)

The *MICROSCOPE* mission was designed to test the weak equivalence principle (WEP), stating the equality between the inertial and the gravitational masses, with a precision of 10^{-15} in terms of the Eötvös ratio η. Its experimental test consisted of comparing the accelerations undergone by two collocated test masses of different compositions as they orbited the Earth, by measuring the electrostatic forces required to keep them in equilibrium. This was done with ultrasensitive differential electrostatic accelerometers onboard a drag-free satellite. The mission lasted two and a half years, cumulating five months worth of science free-fall data, two-thirds with a pair of test masses of different compositions—titanium and platinum alloys—and the last third with a reference pair of test masses of the same composition—platinum. We summarize the data analysis, with an emphasis on the characterization of the systematic uncertainties due to thermal instabilities and on the correction of short-lived events which could mimic a WEP violation signal. We found no violation of the WEP, with the Eötvös parameter of the titanium and platinum pair constrained to $\eta(\mathrm{Ti},\mathrm{Pt}) = [-1.5 \pm 2.3(\mathrm{stat}) \pm 1.5(\mathrm{syst})] \times 10^{-15}$ at 1σ in statistical errors.

DOI: 10.1103/PhysRevLett.129.121102

General relativity (GR) offers a remarkable description of gravitational interactions, successfully tested in the anomalous precession of the perihelion of Mercury, the bending of light in a gravitational field, the gravitational redshift, the Shapiro time delay and the change in the periods of binary pulsars from the emission of gravitational waves [1–10]. Gravitational waves from the coalescence of neutron stars and very massive black holes have been observed recently, providing evidence for the existence of black holes and ruling out many beyond-GR models [11–19].

A building block of general relativity is the equivalence principle (EP), according to which all bodies fall in the same way in a gravitational field when no other forces are acting on them, independently of their masses and internal constitutions. First observed by Galileo and Newton and tested by Eötvös *et al.* at the 5×10^{-9} level [20], the

 © 2022 American Physical Society

universality of free fall was elevated to a principle by Einstein, the weak equivalence principle (WEP), taken as a cornerstone of general relativity [21].

Still the above tests of GR are classical, i.e., not involving quantum physics. But one does not know how to cast GR into a consistent quantum theory, even if several approaches, including most notably string theories [22], have been developed to tackle this problem. At the conceptual level, also, physicists have been dreaming of a unified theory including strong, electromagnetic, and weak interactions as well as gravity.

As GR cannot be considered as a complete theory, and in view of other questions such as the nature of dark energy [23,24] and dark matter [25,26], it is important to test as precisely as possible the EP. Both the need to complete GR if it is to be turned into a satisfactory quantum theory, and the desire for a unified description of interactions, lead to consider the possibility of new long-ranged interactions and forces, that could lead to very small apparent violations of the EP.

Thereby, a test of the EP appears as a test of one of the basic principles of GR, and also serves as a search for new interactions. While gravity is supposed to be mediated by the (still hypothetical) spin-2 graviton, extremely weak new forces could be mediated by very light or massless spin-0 or spin-1 bosons, that may be thought of as part of a completion of GR. Such EP-violating spin-0 bosons, like the dilaton or other dilaton-like particles, tend to appear within string theories [27–37]. A spin-1 boson U associated with an extension of the standard model gauge group is expected to couple to a combination of baryonic, leptonic (or B-L within grand unification) and electromagnetic currents (with possibly axial couplings, of no effects here) [38,39].

The WEP has been intensively tested throughout the past four centuries [1,20,40–43], and verified to a precision of 2×10^{-13} in the first decade of the 21st century [44–46]. This precision has been increased by 1 order of magnitude (2×10^{-14}) with the first results of the *MICROSCOPE* mission in 2017 [47,48], taking advantage of space quietness [49] and of new instrument capabilities [50]. At about the same time, over 48 years of lunar laser ranging (LLR) data allowed for a 7.1×10^{-14} precision [51]. We report here the final *MICROSCOPE* mission results, setting the tightest bound on the validity of the WEP achieved to date, also providing improved constraints on additional new forces [52–54].

The *MICROSCOPE* space mission was designed following developments of the satellite test of the equivalence principle (STEP) [55,56], built from Chapman's seminal proposal to test the WEP in the Earth orbit as early as the 1970s [49]. Albeit less ambitious than STEP, it was designed to test the WEP in space in terms of the Eötvös ratio

$$\eta_{A,B} = 2\frac{a_A - a_B}{a_A + a_B} \tag{1}$$

$$\simeq \left(\frac{m_g}{m_i}\right)_A - \left(\frac{m_g}{m_i}\right)_B = \delta(A,B), \tag{2}$$

where a_A and a_B are the accelerations of two free-falling test bodies A and B, and m_g and m_i their gravitational and inertial masses, respectively. Equation (2) defines the approximated Eötvös ratio to be estimated by *MICROSCOPE* [57,58]. The bodies are two concentric hollow cylindrical test masses controlled with electrostatic forces in a differential accelerometer. Any difference in the forces required to keep the two test masses in relative equilibrium would provide evidence for an apparent violation of the WEP, originating from an intrinsic violation, or as an effect of extremely small new forces [59]. *MICROSCOPE* includes two such differential accelerometers called sensor units: in the first one (SUREF), the two test masses have the same composition (Pt:Rh alloy); in the second one (SUEP), they have different compositions [PtRh(90/10) and TiAlV(90/6/4) alloys]. The former serves as a reference instrument, while the latter is used to test the WEP. The test masses' characteristics are summarized in Table I, and details about the instrument can be found in Refs. [47,48,60]. The payload was integrated in a drag-free CNES microsatellite able to provide the experiment with a very quiet environment [61]. *MICROSCOPE* was launched from Kourou on April 25, 2016 and set into a sun-synchronous, dawn-dusk orbit to optimize its thermal stability. The mission ended on October 18, 2018. Reference [62] presents the mission scenario.

The experimental observable relevant to the test of the WEP is the difference between the electrostatic accelerations exerted on the inner (labeled 1) and the outer (labeled 2) test masses of a given sensor unit $\vec{\Gamma}_d^{\,\mathrm{meas}} \equiv \vec{\Gamma}_1^{\,\mathrm{meas}} - \vec{\Gamma}_2^{\,\mathrm{meas}}$. It is directly related to the Eötvös ratio $\eta(2,1) \approx \delta(2,1)$ and to the

TABLE I. Main test-mass physical properties measured in the laboratory before integration in the instrument.

Measured parameters at 20 °C	SUREF Inner mass Pt/Rh	SUREF Outer mass Pt/Rh	SUEP Inner mass Pt/Rh	SUEP Outer mass Ti/Al/V
Mass (kg)	0.401 533	1.359 813	0.401 706	0.300 939
Density ($\mathrm{g\,cm^{-3}}$)	19.967	19.980	19.972	4.420

various forces acting on the satellite (see Ref. [59] for a detailed derivation). In the instrument's reference frame,

$$\vec{\Gamma}_d^{\text{meas}} \simeq \vec{K}_{0,d} + [A_c]\{([T]-[\text{In}])\vec{\Delta} - 2[\Omega]\dot{\vec{\Delta}} - \ddot{\vec{\Delta}} + \delta(2,1)\vec{g}_{\text{sat}}\} + 2[A_d]\vec{\Gamma}_c^{\text{app}} + 2[C_d]\dot{\vec{\Omega}} + \vec{n}_d, \quad (3)$$

where $\vec{K}_{0,d}$ is a differential bias, $\vec{\Delta}$ connects the center of the inner mass to that of the outer mass, $[T]$ is the gravity gradient tensor in the satellite frame, $[\text{In}] = [\dot{\vec{\Omega}}] + [\vec{\Omega}][\vec{\Omega}]$ is the gradient of inertia, with $[\vec{\Omega}]$ the satellite's angular velocity matrix, $\vec{g}_{\text{sat}}$ is the Earth's gravity acceleration at the center of the satellite, $\vec{\Gamma}_c^{\text{app}}$ is the mean acceleration applied on both masses, $[C_d]$ is the differential-mode linear-to-angular acceleration coupling matrix, $\vec{n}_d$ is the noise, and dots denote differentiation with respect to time. Finally, the common- and differential-mode sensitivity matrices $[A_c]$ and $[A_d]$ are defined from the instrument's scale factors and test-mass reference frame defects. Those parameters are more fully described in Table II of Ref. [47] and in Refs. [48,59,63].

The test of the WEP is performed along the longitudinal axis of the test masses, designed to be the most sensitive. Data analysis thus deals with the differential acceleration (3) projected along the longitudinal, sensitive x axis of the instrument. Reference [59] provides the measurement equation projected on this axis.

The satellite can be spun around the normal y axis to the orbital plane and oppositely to the orbital motion in order to increase the frequency of the Earth's gravity modulation. In this case, in the satellite frame, the Earth's gravity field rotates at the sum of the orbital and spin frequencies. A WEP violation would give a signal modulated at this frequency, denoted f_{EP}. The frequencies used during the mission are listed in Table II. Reference [62] introduces the concept of sessions: WEP test sessions last several days and are defined by their spin frequencies, while calibration sessions are short and allow us to estimate instrumental parameters.

The analysis of first results in Refs. [47,48] used one 120-orbit session on SUEP to obtain $\delta(\text{Ti},\text{Pt}) = [-1 \pm 9(\text{stat}) \pm 9(\text{syst})] \times 10^{-15}$ at 1σ statistical uncertainty. No calibration was used, and systematic errors were dominated by thermal effects, for which an upper bound was used.

TABLE II. Frequencies of interest.

	Frequency ($\times 10^{-3}$ Hz)	Comment
f_{orb}	0.168 18	Mean orbital frequency
f_{spin_2}	$\frac{9}{2} f_{\text{orb}} = 0.756\,81$	Spin rate frequency 2 (V2 mode)
f_{spin_3}	$(35/2) f_{\text{orb}} = 2.943\,15$	Spin rate frequency 3 (V3 mode)
f_{EP_2}	0.924 99	EP frequency in V2 mode
f_{EP_3}	3.111 33	EP frequency in V3 mode
f_{cal}	1.228 48	Calibration frequency

Improvements were then expected in the pursuit of the mission and its data analysis.

We report here the final results of the *MICROSCOPE* mission, based on eighteen sessions for SUEP and nine sessions for SUREF, with all data calibrated and systematics now fully characterized [63,64]. Reference [65] presents the methods used for data analysis, and Ref. [66] details their results on the actual data. The main aspects of the data and its analysis are summarized below.

A handful of sessions were discarded because of nonlinearities at the beginning of the mission, before the control loop's electronics was upgraded. A few others were discarded because of rare anomalies. The results presented in this Letter were then obtained from eighteen sessions on SUEP and nine on SUREF, including two with both SUs switched on together [66]. Hereafter, we first describe the data analysis methods before discussing the actual in-flight estimation of instrumental parameters and presenting the Eötvös parameter determination.

Each in-flight calibration session is dedicated to estimating one or two parameters and designed so that the signals sourced by those parameters have a favourable signal-to-noise ratio. Using a Markov chain Monte Carlo (MCMC) technique on nine sessions, we showed that it is possible to cumulate sessions and estimate all parameters simultaneously from Eq. (3). This unpublished study, based on Ref. [67], used the data of Ref. [47] and gave results consistent with those of the technique described below. Indeed, instead of using a CPU-expensive MCMC method, we use the fact that parameters are almost independent to simplify and better control the estimation process. This is done via the following iterative method based on the ADAM (Accelerometric Data Analysis for *MICROSCOPE*) code to estimate parameters in the frequency domain. The method is presented and applied to numerical simulations in Ref. [65].

When projected on the x axis, the measurement equation (3) is of the form $\Gamma_{d,x} = f(p_k, t) + n_{d,x}$, where p_k are parameters and the time dependence is related to measured or modeled signals $s_i(t)$. For each session, the data provide us with $\Gamma_{d,x}$ and all $s_i(t)$, allowing for the estimation of the parameters p_k. Moreover, *a priori* values $p_{k,0}$ (either measured on ground or estimated during an earlier in-flight calibration session) are used to correct the measurement for the corresponding signals and to refine the estimation of some parameters p_{ke}.

In practice, instrumental defects are parametrized by the $\vec{K}_{0,d}$ and $\vec{\Delta}$ vectors, as well as the $[A_d]$, $[A_c]$, and $[C_d]$ matrices in Eq. (3). Note that only some of their components impact the projected acceleration. Reference [59] details how they affect the measurement and Ref. [63] shows how they were estimated in flight and evolve in time. The estimation of Δ_x and Δ_z takes advantage of their couplings with the Earth's gravity gradient, whose strong line at $2f_{\text{EP}}$ allows for a direct determination in science data

TABLE III. Mean estimated values of the off-centerings' components and of the first row of the $[A_d]$ matrix estimated in flight [63]. The off-centerings' components Δ_x and Δ_z correspond to sessions within a limited temperature range.

	SUEP	SUREF
Δ_x (μm)	19.998 ± 0.009	-35.884 ± 0.005
Δ_y (μm)	-8.19 ± 0.09	5.89 ± 0.05
Δ_z (μm)	-5.605 ± 0.009	5.712 ± 0.005
a_{d11} ($\times 10^{-3}$)	8.5 ± 0.2	-14.6 ± 0.2
a_{d12} ($\times 10^{-5}$ mrad)	-25.6 ± 0.5	-3.5 ± 1.5
a_{d13} ($\times 10^{-5}$ mrad)	13.6 ± 0.9	-9.1 ± 0.3
$K_{2d,xx}$	-1037 ± 4800	2409 ± 1650

from an accurate Earth's gravity model [68,69]. Dedicated 5-orbit sessions were used to measure Δ_y, where the satellite was oscillated about the z axis at frequency $f_{\rm cal}$ to create a measurable signal driven by Δ_y at $f_{\rm cal}$. The elements of the first row of the $[A_d]$ matrix a_{d1i} were measured by shaking the satellite at frequency $f_{\rm cal}$ along each axis (x to measure a_{d11}, y for a_{d12}, and z for a_{d13}) in order to drive a measurable signal dependent on those parameters. The a_{d11} sessions also allowed for a measurement of the differential quadratic factor $K_{2d,xx}$ at $2f_{\rm cal}$. Although we found a slight correlation of Δ_x and Δ_z with temperature, the other parameters remained roughly constant during the mission [63]. Table III lists their mean values.

Once the above iterative process had converged (typically in two to three iterations), we estimated the Eötvös parameter on calibrated data following the corrected measurement equation

$$\Gamma_{d,x}^{\rm corr} = \tilde{b}'_{d,x} + \delta_x g_x + \delta_z g_z + \Delta_x S_{xx} + \Delta_z S_{xz} + n_{d,x}, \qquad (4)$$

which is the core model fitted to the data, where $\tilde{b}'_{d,x}$ is the bias. In addition to the Eötvös parameter δ_x we also estimated the amplitude δ_z of a signal proportional to g_z (varying also at $f_{\rm EP}$ but in quadrature with g_x) and the components Δ_x and Δ_z of the apparent off centering.

Additionally, spurious events can be spotted in the data. "Glitches" are short-lived events, most probably due to crackles of the satellite's multilayer insulator [70]. Glitches occur quasiperiodically and can impart a signal at $f_{\rm EP}$. Although numerical models do not allow for the estimation of the level of this signal, we noticed that removing glitches from sessions with a strong signal at $f_{\rm EP}$—statistically inconsistent with other sessions—decreases the signal, hinting at a significant effect from glitches on the Eötvös parameter estimation. Therefore, to counteract their direct effect on *MICROSCOPE*'s WEP measurement, we masked them as follows. We used a standard recursive σ-clipping technique—σ being the standard deviations of the data—to search for outliers, defined as points that deviate by more than (i) 4.5σ from the moving average of the data and (ii) more than 3σ from the moving average of the high-frequency-filtered data. We then mask one (15) second(s) before (after) each outlier to make sure that the transient regime was always removed [62,66]. Masked glitches thus behaved as "missing" data, so that data became unevenly sampled in time, thereby hampering ADAM's fit in the frequency domain [71,72].

We tackled this difficulty with the M-ECM (modified-expectation-conditional-maximization [73]) technique; it maximizes the likelihood of available data through the estimation of missing data by their conditional expectation, based on the circulant approximation of the complete data covariance. We showed in Ref. [73] that it faithfully reconstructs the noise power spectral density and provides unbiased estimates of parameters. Finally, we added and correctly measured mock WEP violation signals in the data to make sure that this procedure does not affect a possible real WEP violation signal.

M-ECM also fills gaps, and we can then use ADAM to cross-check M-ECM's estimates of the Eötvös parameter for each session. We also use it to combine all sessions and infer the overall constraint given below.

In addition to glitches, rare jumps in the differential acceleration can be spotted, mostly on SUREF [66]. These jumps are not simple discontinuities, but appear as unsteady transitions between two stable states. Although hidden in the noise, they perturb the data analysis and must be discarded. Since this amounts to creating gaps of several hundred seconds, we decided to extract "segments" between jumps (or between jumps and any extremity of the session), when such jumps existed (otherwise, we call segment the entire session). Segments are as long as possible and consist of an even number of orbital periods to ensure that potential contamination by signals at frequencies $mf_{\rm orb} + nf_{\rm spin}$ ($m, n \in \mathbb{N}$) are canceled [66].

Figure 1 shows the estimates of the Eötvös parameter for each segment, obtained with M-ECM (blue circles) and ADAM (orange diamonds). The two methods are perfectly consistent. Error bars vary in accordance with the duration of segments and with the spin rate: the higher the spin rate, the lower the error bars, since the noise is minimal for the highest spin rate, see Ref. [66]. The black lines and gray areas show the combined constraints and their 68% confidence region [65,66], $\delta(\mathrm{Pt,Pt}) = (0.0 \pm 1.1) \times 10^{-15}$ for SUREF and $\delta(\mathrm{Ti,Pt}) = (-1.5 \pm 2.3) \times 10^{-15}$ for SUEP. Those uncertainties contain statistical errors only. We discuss systematic errors below.

We found that the overall systematics upper bound is 2.3×10^{-15} for SUREF and 1.5×10^{-15} for SUEP, compared to specifications of 0.2×10^{-15} [63]. Except nonlinearity (as discussed in Ref. [64]) and temperature variations (see below), all contributors to the systematics error budget have effects lower than required. For instance, the contribution of the Earth gravity gradient could be canceled by the precise estimation of the test masses off

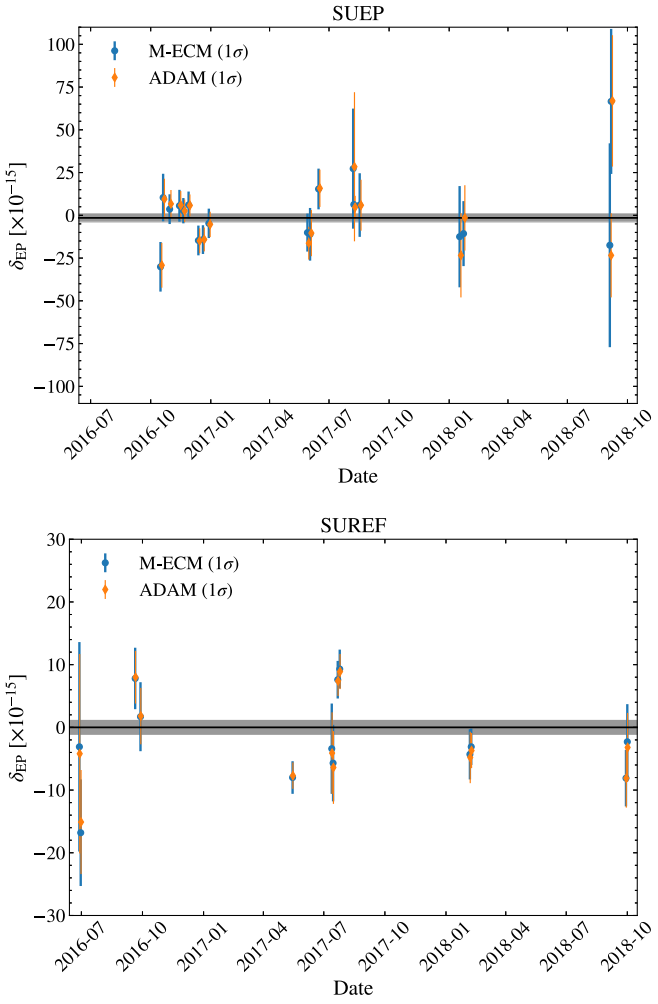

FIG. 1. Eötvös parameter estimates for each segment and overall estimate and its 68% confidence region (black line and gray area). Blue circles show M-ECM's estimates and orange ones ADAM's. Upper panel: SUEP. Lower panel: SUREF. Panels span the same time.

centerings. Local gravity effects were mitigated by a careful design of the satellite and of the instrument [63]. Similarly, we showed in Ref. [63] that magnetic effects, due to the interaction of the test masses with the Earth's magnetic field, were well below the requirements, as expected from the integration of a magnetic shield around the payload. The DFACS performance was much better than expectations, allowing for a residual linear accelerations at f_{EP} smaller than 2×10^{-13} ms^{-2} (6×10^{-14} ms^{-2}) in (out of) the orbital plane, and for residual angular accelerations smaller than 2.5×10^{-11} rad s^{-2}; the related systematic errors are well below the specifications.

Temperature variations are the main source of systematic errors. They induce a differential acceleration through a thermal sensitivity of the SU and of the front end electronics unit (FEEU). Specific sessions were designed to characterize the thermal sensitivity through a periodic stimulus by on-board heaters; the temperature and differential accelerations were finely monitored and compared to provide better estimates of the thermal sensitivities at different frequencies [63,74]. We found a linear frequency dependence for SUEPs thermal sensitivities, but none for SUREFs.

On the other hand, the temperature data during EP sessions only allowed for a pessimistic upper bound since the temperature variations were smaller than the temperature probes noise at f_{EP}. In response to this limitation, additional sessions were devoted to confirm the thermal design of the satellite, in order to show that temperature variations are driven by the Earth's albedo coming through the FEEU radiator's baffle (Fig. 15 of Ref. [63]), inducing a modulation of the temperature at f_{EP} [63]. A first session, based on heating the FEEU panel with local heaters, allowed us to show that the impact of the Earth's albedo on the satellite walls is negligible. In a second session, the satellite was tilted by 30° about its spin axis in inertial mode during 465 orbits (32.3 days) in order to maximize the albedo light entering the FEEU radiator. We found that temperature variations are attenuated by a factor 500 between the FEEU and the SU. Based on the data available (at frequencies lower than 10^{-3} Hz), we took this factor 500 as the lowest limit to compute an upper bound of temperature fluctuations at frequencies higher than 10^{-3} Hz, in particular at f_{EP}, where temperature probes allow for a measurement of the FEEU temperature variations but not of the SU's, since it is below the probe's noise [63].

Putting these results together, *MICROSCOPE*'s new constraint on the validity of the WEP is

$$\eta(\mathrm{Ti,Pt}) = [-1.5 \pm 2.3(\mathrm{stat}) \pm 1.5(\mathrm{syst})] \times 10^{-15}, \qquad (5)$$

where the statistical error is given at 1σ, and where we identified the measured, approximated Eötvös ratio δ with the exact one η. This result is close to the 10^{-15} precision for which the mission was designed, and improves our previous constraints [47] by a factor 4.6. The reference instrument provided a null result, $\eta(\mathrm{Pt,Pt}) = [0.0 \pm 1.1(\mathrm{stat}) \pm 2.3(\mathrm{syst})] \times 10^{-15}$, showing no sign of unaccounted systematic errors in Eq. (5). As expected, SUREF's statistical error is smaller than SUEP's because it is more sensitive.

Beside constraining the validity of the WEP to an unprecedented level, *MICROSCOPE* also allows for unprecedented constraints on topics as various as Lorentz invariance [75], long-range interactions [52–54,76,77], or dark matter searches [78]. It also paves the way to new, more ambitious experiments to test GR in space [79]. The analyses presented in this Letter and in Refs. [47,48] provide essential feedback for future upgrades on the payload and satellite sides that can lead to the next-generation *MICROSCOPE* mission. In particular, the gold wire allowing for the test masses charge management should be replaced by a

contactless device, such as the one proven to work in space in LISA Pathfinder [80–82]. Glitches should be reduced to a minimum, e.g., by tightening the requirement on the crackles of the satellite's coating, or their effect should be better understood, e.g., through a better understanding of the full transfer function of the satellite instrument system, so that it can be efficiently corrected for. Furthermore, a better thermal stability and thermal characterization of the system will allow us to beat the thermal systematics. With these upgrades, not only should it be possible to reach a 10^{-17} precision on the Eötvös ratio, but also to provide unprecedented constraints on topics as various as Lorentz invariance [77], long-range interactions [52,53], or dark matter searches [78].

The authors express their gratitude to all the different services involved in the mission partners and in particular CNES, the French space agency in charge of the satellite. This work is based on observations made with the T-SAGE instrument, installed on the CNES-ESA-ONERA-CNRS-OCA-DLR-ZARM *MICROSCOPE* mission. ONERA authors work is financially supported by CNES and ONERA fundings. Authors from OCA, Observatoire de la Côte d'Azur, have been supported by OCA, CNRS, the French National Center for Scientific Research, and CNES. ZARM authors's work is supported by the DLR, German Space Agency, with funds of the BMWi (FKZ 50 OY 1305), and by the Deutsche Forschungsgemeinschaft DFG (LA 905/12-1). The authors would like to thank the Physikalisch-Technische Bundesanstalt institute in Braunschweig, Germany, for their contribution to the development of the test masses with funds of CNES and DLR.

[*]Deceased.
[†]Gilles.Metris@oca.eu
[‡]manuel.rodrigues@onera.fr
[§]Present address: CEA, Centre de Saclay, IRFU/DPhP, 91191 Gif-sur-Yvette, France.
[‖]Present address: DLR, Institute for Satellite Geodesy and Inertial Sensing, Am Fallturm 9, D-28359 Bremen, Germany.
[¶]Present address: AIRBUS Defence and Space, F-31402 Toulouse, France.
[**]Present address: KINEIS, F-31520 Ramonville Saint-Agne, France.
[††]Present address: GERADTS GMBH, Kleiner Ort 8, D-28357 Bremen, Germany.

[1] C. M. Will, The confrontation between general relativity and experiment, Living Rev. Relativity **17**, 4 (2014).
[2] C. M. Will, *Theory and Experiment in Gravitational Physics*, 2nd ed. (Cambridge University Press, Cambridge, England, 2018).
[3] G. M. Tino, L. Cacciapuoti, S. Capozziello, G. Lambiase, and F. Sorrentino, Precision gravity tests and the Einstein Equivalence Principle, Prog. Part. Nucl. Phys. **112**, 103772 (2020).
[4] B. Bertotti, L. Iess, and P. Tortora, A test of general relativity using radio links with the Cassini spacecraft, Nature (London) **425**, 374 (2003).
[5] H. Hoekstra and B. Jain, Weak gravitational lensing and its cosmological applications, Annu. Rev. Nucl. Part. Sci. **58**, 99 (2008).
[6] A. Fienga, J. Laskar, P. Exertier, H. Manche, and M. Gastineau, Numerical estimation of the sensitivity of INPOP planetary ephemerides to general relativity parameters, Celestial Mech. Dyn. Astron. **123**, 325 (2015).
[7] P. Delva, N. Puchades, E. Schönemann, F. Dilssner, C. Courde, S. Bertone, F. Gonzalez, A. Hees, C. Le Poncin-Lafitte, F. Meynadier, R. Prieto-Cerdeira, B. Sohet, J. Ventura-Traveset, and P. Wolf, Gravitational Redshift Test Using Eccentric Galileo Satellites, Phys. Rev. Lett. **121**, 231101 (2018).
[8] S. Herrmann, F. Finke, M. Lülf, O. Kichakova, D. Puetzfeld, D. Knickmann, M. List, B. Rievers, G. Giorgi, C. Günther, H. Dittus, R. Prieto-Cerdeira, F. Dilssner, F. Gonzalez, E. Schönemann, J. Ventura-Traveset, and C. Lämmerzahl, Test of the Gravitational Redshift with Galileo Satellites in an Eccentric Orbit, Phys. Rev. Lett. **121**, 231102 (2018).
[9] R. Abuter *et al.* (GRAVITY Collaboration), Detection of the Schwarzschild precession in the orbit of the star s2 near the galactic centre massive black hole, Astron. Astrophys. **636**, L5 (2020).
[10] M. Kramer *et al.*, Strong-Field Gravity Tests with the Double Pulsar, Phys. Rev. X **11**, 041050 (2021).
[11] B. P. Abbott *et al.*, Observation of Gravitational Waves from a Binary Black Hole Merger, Phys. Rev. Lett. **116**, 061102 (2016).
[12] B. P. Abbott, R. Abbott, T. D. Abbott, F. Acernese, K. Ackley, C. Adams, T. Adams, P. Addesso, R. X. Adhikari, V. B. Adya *et al.*, GW170817: Observation of Gravitational Waves from a Binary Neutron Star Inspiral, Phys. Rev. Lett. **119**, 161101 (2017).
[13] P. Brax, C. Burrage, and A.-C. Davis, The speed of Galileon gravity, J. Cosmol. Astropart. Phys. 03 (2016) 004.
[14] L. Lombriser and A. Taylor, Breaking a dark degeneracy with gravitational waves, J. Cosmol. Astropart. Phys. 03 (2016) 031.
[15] L. Lombriser and N. A. Lima, Challenges to self-acceleration in modified gravity from gravitational waves and large-scale structure, Phys. Lett. B **765**, 382 (2017).
[16] T. Baker, E. Bellini, P. G. Ferreira, M. Lagos, J. Noller, and I. Sawicki, Strong Constraints on Cosmological Gravity from GW170817 and GRB 170817A, Phys. Rev. Lett. **119**, 251301 (2017).
[17] P. Creminelli and F. Vernizzi, Dark Energy after GW170817 and GRB170817A, Phys. Rev. Lett. **119**, 251302 (2017).
[18] J. M. Ezquiaga and M. Zumalacárregui, Dark Energy After GW170817: Dead Ends and the Road Ahead, Phys. Rev. Lett. **119**, 251304 (2017).
[19] J. Sakstein and B. Jain, Implications of the Neutron Star Merger GW170817 for Cosmological Scalar-Tensor Theories, Phys. Rev. Lett. **119**, 251303 (2017).

[20] L. Eötvös, D. Pekár, and E. Fekete, Beiträge zum Gesetz der Proportionalität von Trägheit and Gravität, Ann. Phys. (N. Y.) **373**, 11 (1922), English translation in Annales Universitatis Scientiarium Budapestiensis de Rolando Eötvös Nominate, Sectio Geologica, 7, 111, 1963.

[21] A. Einstein, über das Relativitätsprinzip und die aus demselben gezogene Folgerungen, Jahrb. Radioakt. Elektron. **4**, 411 (1907); English translation in *The Collected Papers of Albert Einstein Volume 2*, (Princeton University Press, Princeton, NJ, 1989), doc.47.

[22] K. Becker, M. Becker, and J. H. Schwarz, *String Theory and M-Theory: A Modern Introduction* (Cambridge University Press, Cambridge, England, 2006).

[23] A. G. Riess *et al.*, Observational evidence from supernovae for an accelerating universe and a cosmological constant, Astron. J. **116**, 1009 (1998).

[24] S. Perlmutter *et al.* (The Supernova Cosmology Project), Measurements of Ω and Λ from 42 high-redshift supernovae, Astrophys. J. **517**, 565 (1999).

[25] F. Zwicky, Die Rotverschiebung von extragalaktischen Nebeln, Helv. Phys. Acta **6**, 110 (1933).

[26] V. C. Rubin and W. K. Ford, Jr., Rotation of the Andromeda Nebula from a spectroscopic survey of emission Regions, Astrophys. J. **159**, 379 (1970).

[27] T. Damour and A. M. Polyakov, The string dilation and a least coupling principle, Nucl. Phys. **B423**, 532 (1994).

[28] T. Damour, F. Piazza, and G. Veneziano, Runaway Dilaton and Equivalence Principle Violations, Phys. Rev. Lett. **89**, 081601 (2002).

[29] J. Khoury and A. Weltman, Chameleon cosmology, Phys. Rev. D **69**, 044026 (2004).

[30] J. Khoury and A. Weltman, Chameleon Fields: Awaiting Surprises for Tests of Gravity in Space, Phys. Rev. Lett. **93**, 171104 (2004).

[31] T. Clifton, P. G. Ferreira, A. Padilla, and C. Skordis, Modified gravity and cosmology, Phys. Rep. **513**, 1 (2012).

[32] A. Joyce, B. Jain, J. Khoury, and M. Trodden, Beyond the cosmological standard model, Phys. Rep. **568**, 1 (2015).

[33] A. I. Vainshtein, To the problem of nonvanishing gravitation mass, Phys. Lett. **39B**, 393 (1972).

[34] E. Babichev, C. Deffayet, and R. Ziour, k-MOUFLAGE Gravity, Int. J. Mod. Phys. D **18**, 2147 (2009).

[35] K. Hinterbichler and J. Khoury, Screening Long-Range Forces through Local Symmetry Restoration, Phys. Rev. Lett. **104**, 231301 (2010).

[36] P. Brax, C. Burrage, and A.-C. Davis, Screening fifth forces in k-essence and DBI models, J. Cosmol. Astropart. Phys. 01 (2013) 020.

[37] C. Burrage and J. Sakstein, Tests of chameleon gravity, Living Rev. Relativity **21**, 1 (2018).

[38] P. Fayet, The fifth force charge as a linear combination of baryonic, leptonic (or B-L) and electric charges, Phys. Lett. B **227**, 127 (1989).

[39] P. Fayet, Extra U(1)'s and new forces, Nucl. Phys. **B347**, 743 (1990).

[40] E. Fischbach and C. L. Talmadge, *The Search for Non-Newtonian Gravity* (Springer-Verlag, New York, 1999), p. 58.

[41] P. G. Roll, R. Krotkov, and R. H. Dicke, The equivalence of inertial and passive gravitational mass, Ann. Phys. (N.Y.) **26**, 442 (1964).

[42] R. H. Dicke, *Gravitation and the Universe* (Philadelphia American Philosophical Society, 1970).

[43] V. Braginsky and V.-I. Panov, Verification of the equivalence of inertial and gravitational mass, Zh. Eksp. Teor. Fiz. **61**, 873 (1971).

[44] S. Schlamminger, K.-Y. Choi, T. A. Wagner, J. H. Gundlach, and E. G. Adelberger, Test of the Equivalence Principle Using a Rotating Torsion Balance, Phys. Rev. Lett. **100**, 041101 (2008).

[45] T. A. Wagner, S. Schlamminger, J. H. Gundlach, and E. G. Adelberger, Torsion-balance tests of the weak equivalence principle, Classical Quantum Gravity **29**, 184002 (2012).

[46] J. G. Williams, S. G. Turyshev, and D. H. Boggs, Lunar laser ranging tests of the equivalence principle, Classical Quantum Gravity **29**, 184004 (2012).

[47] P. Touboul *et al.*, *MICROSCOPE* Mission: First Results of a Space Test of the Equivalence Principle, Phys. Rev. Lett. **119**, 231101 (2017).

[48] P. Touboul *et al.*, Space test of the equivalence principle: First results of the *MICROSCOPE* mission, Classical Quantum Gravity **36**, 225006 (2019).

[49] P. K. Chapman and A. J. Hanson, An Eötvös Experiment in Earth Orbit, edited by R. W. Davies, *Proc. Conf. on Experimental Tests of Gravitation Theories* (1970), JPL TM 33-499, 228.

[50] C. W. F. Everitt, T. Damour, K. Nordtvedt, and R. Reinhard, Historical perspective on testing the Equivalence Principle, Adv. Space Res. **32**, 1297 (2003).

[51] V. Viswanathan, A. Fienga, O. Minazzoli, L. Bernus, J. Laskar, and M. Gastineau, The new lunar ephemeris INPOP17a and its application to fundamental physics, Mon. Not. R. Astron. Soc. **476**, 1877 (2018).

[52] J. Bergé, P. Brax, G. Métris, M. Pernot-Borràs, P. Touboul, and J.-P. Uzan, *MICROSCOPE* Mission: First Constraints on the Violation of the Weak Equivalence Principle by a Light Scalar Dilaton, Phys. Rev. Lett. **120**, 141101 (2018).

[53] P. Fayet, *MICROSCOPE* limits for new long-range forces and implications for unified theories, Phys. Rev. D **97**, 055039 (2018).

[54] P. Fayet, *MICROSCOPE* limits on the strength of a new force, with comparisons to gravity and electromagnetism, Phys. Rev. D **99**, 055043 (2019).

[55] J. Mester, R. Torii, P. Worden, N. Lockerbie, S. Vitale, and C. W. F. Everitt, The STEP mission: Principles and baseline design, Classical Quantum Gravity **18**, 2475 (2001).

[56] T. Sumner *et al.*, STEP, equivalence principle, Gravitational experiments, General relativity, Adv. Space Res. **39**, 254 (2007).

[57] P. Touboul, The *MICROSCOPE* mission and its uncertainty analysis, Space Sci. Rev. **148**, 455 (2009).

[58] P. Touboul, G. Métris, V. Lebat, and A. Robert, The MICROSCOPE experiment, ready for the in-orbit test of the equivalence principle, Classical Quantum Gravity **29**, 184010 (2012).

[59] P. Touboul, M. Rodrigues, G. Métris, R. Chhun, A. Robert, Q. Baghi, E. Hardy, J. Bergé, D. Boulanger, B. Christophe, V. Cipolla, B. Foulon, P.-Y. Guidotti, P.-A. Huynh, V. Lebat, F. Liorzou, B. Pouilloux, P. Prieur, and S. Reynaud,

MICROSCOPE mission analysis, requirements and expected performance, arXiv:2012.06472.
[60] F. Liorzou *et al.*, MICROSCOPE instrument description and validation, arXiv:2012.11232.
[61] A. Robert, V. Cipolla, P. Prieur, P. Touboul, G. Métris, M. Rodrigues, Y. André, J. Bergé, D. Boulanger, R. Chhun, B. Christophe, P.-Y. Guidotti, E. Hardy, V. Lebat, T. Lienart, F. Liorzou, and B. Pouilloux, MICROSCOPE satellite and its drag-free and attitude control system, arXiv:2012.06479.
[62] M. Rodrigues, P. Touboul, G. Métris, J. Bedouet, J. Bergé, R. Chhun, B. Christophe, B. Foulon, P.-Y. Guidotti, and A. Robert, MICROSCOPE Mission scenario and ground segment, arXiv:2201.10841.
[63] M. Rodrigues *et al.*, MICROSCOPE: Systematic errors, arXiv:2112.10559.
[64] R. Chhun, E. Hardy, M. Rodrigues, P. Touboul, G. Métris, D. Boulanger, B. Christophe, P. Danto, B. Foulon, P.-Y. Guidotti, P.-A. Huynh, V. Lebat, F. Liorzou, and A. Robert, MICROSCOPE instrument in-flight characterization, arXiv:2102.11087.
[65] J. Bergé, Q. Baghi, E. Hardy, G. Métris, A. Robert, M. Rodrigues, P. Touboul, R. Chhun, P.-Y. Guidotti, S. Pires, S. Reynaud, L. Serron, and J.-M. Travert, MICROSCOPE mission: Data analysis principle, arXiv:2012.06484.
[66] G. Métris (Microscope team), MICROSCOPE WEP test and result, Classical Quantum Gravity (to be published).
[67] S. Vitale *et al.*, Data series subtraction with unknown and unmodeled background noise, Phys. Rev. D **90**, 042003 (2014).
[68] G. Métris, J. Xu, and I. Wytrzyszczak, Derivatives of the gravity potential with respect to rectangular coordinates, Celestial Mech. Dyn. Astron. **71**, 137 (1998).
[69] T. Mayer-Gurr, A. Eicker, and K. H. Ilk, ITG-GRACE02s: A GRACE gravity field derived from short arcs of the satellite's orbit, Proc. First Symp. Int. Grav. Field Ser. 193 (2006).
[70] J. Bergé, Q. Baghi, A. Robert, M. Rodrigues, B. Foulon, E. Hardy, G. Métris, S. Pires, and P. Touboul, MICROSCOPE mission: Statistics and impact of glitches on the test of the weak equivalence principle, arXiv:2012.06485.
[71] Q. Baghi, G. Métris, J. Bergé, B. Christophe, P. Touboul, and M. Rodrigues, Regression analysis with missing data and unknown colored noise: Application to the *MICROSCOPE* space mission, Phys. Rev. D **91**, 062003 (2015).
[72] J. Bergé, S. Pires, Q. Baghi, P. Touboul, and G. Métris, Dealing with missing data: An inpainting application to the *MICROSCOPE* space mission, Phys. Rev. D **92**, 112006 (2015).
[73] Q. Baghi, G. Métris, J. Bergé, B. Christophe, P. Touboul, and M. Rodrigues, Gaussian regression and power spectral density estimation with missing data: The *MICROSCOPE* space mission as a case study, Phys. Rev. D **93**, 122007 (2016).
[74] O. Dhuicque, M. Rodrigues, G. Métris, and P. Touboul, Methods to determine thermal sensitivity of T-SAGE instrument for MICROSCOPE mission, Adv. Space Res. **68**, 1989 (2021).
[75] H. Pihan-le Bars, C. Guerlin, A. Hees, R. Peaucelle, J. D. Tasson, Q. G. Bailey, G. Mo, P. Delva, F. Meynadier, P. Touboul, G. Métris, M. Rodrigues, J. Bergé, and P. Wolf, New Test of Lorentz Invariance Using the *MICROSCOPE* Space Mission, Phys. Rev. Lett. **123**, 231102 (2019).
[76] M. Pernot-Borràs, J. Bergé, P. Brax, and J.-P. Uzan, General study of chameleon fifth force in gravity space experiments, Phys. Rev. D **100**, 084006 (2019).
[77] M. Pernot-Borràs, J. Bergé, P. Brax, and J.-P. Uzan, Fifth force induced by a chameleon field on nested cylinders, Phys. Rev. D **101**, 124056 (2020).
[78] P. W. Graham, D. E. Kaplan, J. Mardon, S. Rajendran, and W. A. Terrano, Dark matter direct detection with accelerometers, Phys. Rev. D **93**, 075029 (2016).
[79] B. Battelier *et al.*, Exploring the foundations of the physical universe with space tests of the equivalence principle, Exp. Astron. **51**, 1695 (2021).
[80] M. Armano *et al.*, Constraints on LISA Pathfinder's self-gravity: Design requirements, estimates and testing procedures, Classical Quantum Gravity **33**, 235015 (2016).
[81] M. Armano *et al.* (LISA Pathfinder Collaboration), Charge-Induced Force Noise on Free-Falling Test Masses: Results from LISA Pathfinder, Phys. Rev. Lett. **118**, 171101 (2017).
[82] M. Armano *et al.* (LISA Pathfinder Collaboration), Precision charge control for isolated free-falling test masses: LISA pathfinder results, Phys. Rev. D **98**, 062001 (2018).